Drag Forces on Falling Objects

Marek Józef Michałowski

———

School of Physics and Astronomy

University of Manchester

Second year laboratory report

May 2021

This experiment was performed in collaboration with ——————————

Abstract

The drag force on an object of a given shape moving through a turbulent fluid with density ρ varies as $F \propto v^2$. The dimensionless constant of proportionality is known as C_d - the coefficient of drag. This experiment aimed to find the values of C_d for muffin cases and cuboid-shaped sponges. The measurements were performed by recording the fall of these objects across a background of known dimensions, converting the recordings into numerical data using the Tracker software and finally analysing it using Python. The resulting values of C_d are 1.08 ± 0.03 for the cuboid shape and 0.47 ± 0.05 for the muffin-case shape. The former result is consistent to one standard deviation with the literature value for a cube moving face-on through a turbulent fluid. The lack of literature values for muffin-case shape made it difficult to estimate its accuracy, however, by comparison with the drag coefficient of a cone, it was deduced to be an underestimation. Additionally, it has been observed that given a constant frontal area the terminal velocity increases proportionally to $\sqrt{m}$, where m is the mass of an object. This is in agreement with the theory.

1 Introduction

The drag coefficient (known as C_d) of an object moving through a turbulent fluid is proportional to the strength of the force opposing its motion. It is of prime importance in areas like aerospace engineering when designing the most fuel-efficient shapes of vehicles. Through detailed study and simulations, engineers can now build shapes with coefficients of drag as small as 0.021 [1], when for example a sphere has its coefficient equal to 0.5 [2].

The goal of this experiment was to investigate the effects of drag forces on freely falling objects. To that end, the coefficients for two shapes - a muffin case and a cuboid sponge - were determined and the relationship between mass and terminal velocity (with other parameters kept constant) investigated.

2 Theory

The two primary types of fluid flow are laminar and turbulent. The former occurs when fluid forms layers of flow that do not intersect or otherwise interact. On the other hand, in turbulent flow, the fluid forms vortices and both the pressure and flow velocity can differ greatly between different points in space and time. Due to this chaotic behaviour, objects moving in a turbulent fluid experience stronger resistance than in the laminar flow. To deduce the type of flow, one can use Reynolds Number (Re), defined as:

$$Re = \frac{\rho L v}{\mu}\,, \tag{1}$$

where ρ and μ are the density and viscosity of the fluid respectively, v is its velocity and L is the characteristic length in question, which in the analysis has been taken to be the longest dimension of an object moving in the fluid [3]. This dimensionless number is an empirical measure and typically flow is turbulent if $Re \geq 10^3$ [2]. One can therefore deduce the type of flow in this experiment. Density and viscosity of air are $\sim 1\,\text{kg m}^{-1}$ and $\sim 10^{-5}$ kg m^{-1} s^{-1} [2], the velocities reached by the falling objects in this experiment were ~ 1 m s^{-1} and their characteristic lengths were $\sim 10^{-1}$ m. Therefore, Equation (1) yields $Re \simeq 10^4$, confirming that the type of drag experienced by objects in this experiment came from the turbulent flow.

Correspondingly, the force of drag (F_d) acting on the objects had the form:

$$F_d = \frac{1}{2} C_d \rho A v^2\,, \tag{2}$$

where C_d and ρ are the coefficient of drag and density of the air as before, while v and A are the velocity and the frontal area of the object in question. Then, using Newton's 2^{nd} law:

$$m\ddot{y} = mg - \rho V g - F_d\,, \tag{3}$$

where m, V and y are the mass, volume and displacement of the object, while g is the acceleration due to gravity. The second term on the right-hand side comes from the buoyant force. To make the equation easier to solve one can divide both sides by m, then define $g' \equiv g(1 - \frac{\rho V}{m})$ and $S^2 \equiv \frac{2C_d \rho A g'}{m}$. Doing this yields:

$$\ddot{y} = g'(1 - \frac{S^2 \dot{y}^2}{4g'^2}), \tag{4}$$

which can be integrated to give the expressions for velocity and displacement:

$$\dot{y} = \frac{2g'}{S} \tanh \frac{St}{2} \tag{5}$$

and

$$y = \frac{4g'}{S^2} \ln(\cosh \frac{St}{2}), \tag{6}$$

where t is the time elapsed since the object began to fall [3].

Finally, Equation (5) can be used to find the expression for terminal velocity by taking the limit $t \to \infty$ which shows its square-root dependence on mass:

$$v_{ter} = m^{1/2} \sqrt{2g'/C_d \rho A}. \tag{7}$$

3 Methodology

3.1 Recording the Video Data

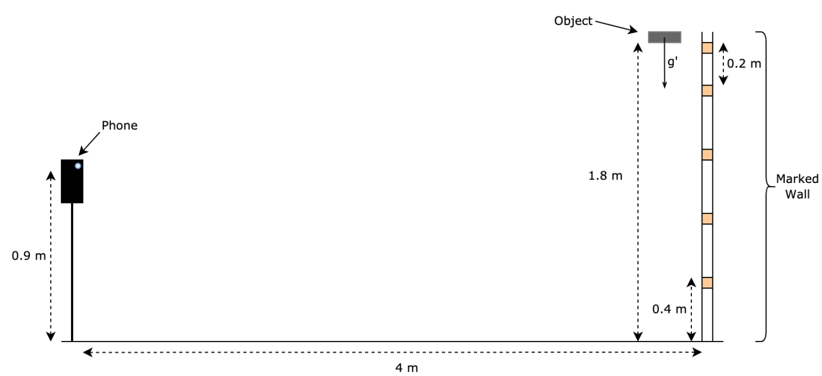

Figure 1: A diagram showing the experimental setup, including the exact distances and positions

The setup of the experiment was designed with three key goals: (a) providing enough height for the objects to reach close to terminal velocity, (b) reducing the image distortion and (c) obtaining enough detail in the video to reduce the error in position. Goal (a) was limited mainly by the height of the room and safety concerns. A series of initial trials established that 1.8 m is both safe for the experimenter and suffices in most cases, as seen in Figure 1.

However, goals (b) and (c) are generally in opposition with one another. To decrease distance distortion in the image, one wants to put the lens as far away as possible so that most rays come from the wall at around the same angle. On the other hand, a camera must be placed close to the wall to register the most detail in the video. Fortunately, the phone camera used was capable of recording videos at 4K in 60 frames per second, which allowed to place it at a distance of 4 m away from the wall as seen in Figure 1 and it still provided a high-resolution image. The lens was then placed on a camera stand at a height of 0.9 m (half the height of the drop) to minimise the length distortion over the whole fall. Using a tape measure, sticker markers were carefully placed every 0.4 m on the wall (except for the top-most one which was placed 0.2 m above the previous). Tracker software was then used to see how much the distances have been distorted, which showed a difference of at most 0.003 m from the actual distances. This level of distortion was therefore a negligible source of error compared to other factors like the random wobble of an object as it was falling.

Measurements were always taken in the same way. First, the recording was started and the experimenter stood with the object placed at the height of ~ 1.8 m as close to the wall as possible without touching. Then the object was released (always facing the same way) by only letting go with the fingers. Finally, after the object touched the ground the experimenter moved again and stopped the recording. The windows and doors in the room were closed to minimise air movement and all lights were turned on to provide better exposure. Nonetheless, many trials ended up with the object turning mid-air which naturally affected its frontal area and C_d. Such trials were discarded as faulty and a new trial was recorded instead.

A total of 14 trials were recorded for the sponges. The frontal area was kept constant (the biggest side of a sponge), but each trial contained a different number of sponges stacked together. 9 trials contained a light, thin, plastic stick going through the centres of sponges to hold them better together and add a different amount of mass. The stick never pierced the bottom-most sponge the reduce the effect a central hole could have on drag. 4 trials contained half a sponge on the very top as well as a stick. Half a sponge was never dropped in its own trial as the frontal area was different from the rest. For muffin cases, there were 5 sets of 3 trials. Each set had its mass kept constant by using the same number of muffin cases stacked together. The number of muffin cases were increased from 1 in the first trial to 5 in the last.

	Mass (g)	Uncertainty in Mass (g)	Area (cm^2)	Uncertainty in Area (cm^2)
Sponge	2.3	0.2	83.2	0.7
Plastic Stick	1.0	0.2	—	—
Muffin Case	0.333	0.066	44	9

Table 1: The masses and areas of objects used in the experiment.

The relevant values of masses and areas can be seen in Table 1. The area of the stick was never measured since it was never directly in contact with the airflow. The high uncertainty in the frontal area of a muffin case seen in the table can be attributed to its irregular shape. Each object had a minuscule mass, which could hardly be weighted precisely by the scale. Hence all masses have been measured by stacking a high number of the given object on a kitchen scale and then dividing the result by their amount.

3.2 Obtaining the Numerical Data

Once the videos of all trials were recorded, they were uploaded to Tracker software. The origin of coordinates was always placed at the starting position of the objects and the axis parallel to the markings on the wall (positive direction being defined downwards). The exact starting time contained some human error. To minimise its random component, the starting frame was chosen to be the first one which is directly followed by a movement downwards, no matter how small. The remaining major error would therefore by systematic and should matter less in the fitting process.

The actual tracking was performed automatically by the software. It used pattern matching to find the centre of a falling object at each successive frame. This process became more accurate when the whole object and some of the background was used as a pattern to be matched, at a cost of a longer computation time. This is because as the object started moving faster, it became more blurry, but the overall centre of the pattern tended to be reliably found by the software to within 1 cm. On the other hand, the error in the time of a frame was taken to be negligible.

The raw numerical data was then analysed in Python. Equation (6) contains two free parameters when the data is fit: g' and S^2. The former was calculated using the central Euler difference approximation:

$$g' \simeq \frac{2y_{i-2} - y_{i-1} + y_i - y_{i+1} + 2y_{i+2}}{7(\delta t)^2}\,, \tag{8}$$

where y_i is the vertical displacement of the object in the ith frame and the time difference between consecutive frames is $\delta t = 0.017$ s. Equation (8) was applied to the 3^{rd}, 4^{th} and 5^{th} frame when the effect of drag was assumed to be small. Then the average was taken and the uncertainty given as the standard error. This reduced the number of free parameters in Equation (6) to one, making fitting in Python more efficient. The value of S^2 was obtained directly from the fit and its error propagated using the partial differential approach. Afterwards, the same was done to calculate the value and error of C_d from S^2 using its definition. Finally, the terminal velocity v_{ter} of all objects was measured, where again the differential approach was used to propagate the errors.

4 Results and Discussion

The fitted displacement function was plotted alongside original data. Examples of such plots can be seen below, one for two sponges and one for a single muffin case.

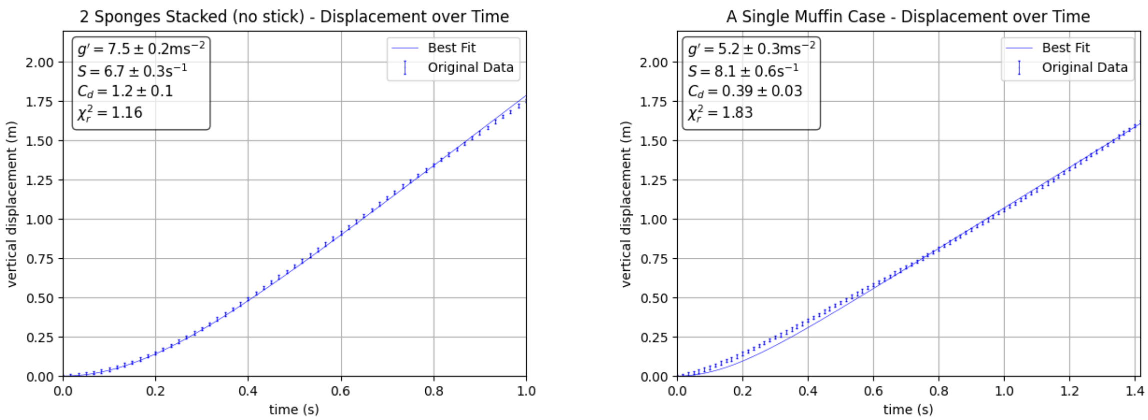

(a) Plot for two sponges falling together.

(b) Plot for a single muffin case falling.

Figure 2: Displacement (m) over time (s) plots of example data including their error bars and best fits.

Both plots in Figure 2 are good representatives of the general trend in their respective groups. Figure 2(a) shows two sponges falling and the best-fit line follows the data points closely, slightly deviating only towards the end. This behaviour was typical of sponges as they tended to change their orientations towards the end of the fall, resulting in a slight change in drag. Nonetheless, the vast majority of the plots had their χ_r^2 of around 1 (same can be seen above), which indicates that equations (6) and (7) used together are very good at modelling the fall of sponges. Consequently, the value of the coefficient of drag, which follows directly from the fitting parameters, can be expected to be accurate for the cuboid shape.

Meanwhile, Figure 2(b) shows the typical deviation of muffin cases from the line of best-fit right from the beginning. Its value of χ_r^2 is larger than that of sponges, sitting at 1.83. This is typical for muffin cases, whose χ_r^2 is usually between 2 and 3. The most likely explanation is that the cases start experiencing a significant force of drag much earlier than sponges do. This can be attributed to their smaller mass per single unit (0.33 g $<$ 2 g), which causes the weight force to be overwhelmed much quicker. This then leads to the estimation of g' as given in Equation (8) to be less accurate since it depends on the assumption that drag is insignificant for the first 7 frames. A naive fix would be to only use the first 5 frames (which is the bare minimum for the central Euler difference used here). However, when that was attempted the resulting fit was often even worse due to random variations. In another attempt, forward and backward Euler differences were tried but resulted in even more random values. Therefore, averaging 3 separate values of g' proved to be more reliable and accurate, even though it had an obvious downside.

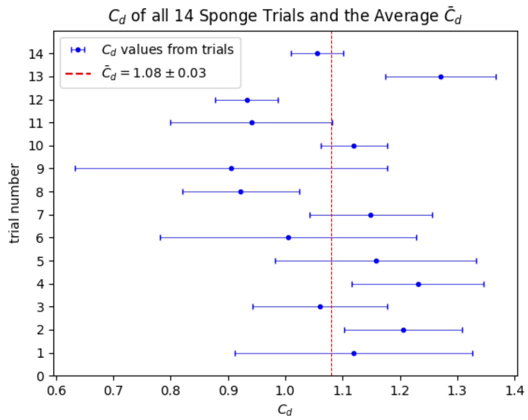

(a) Forest plot of measured C_d for sponges.

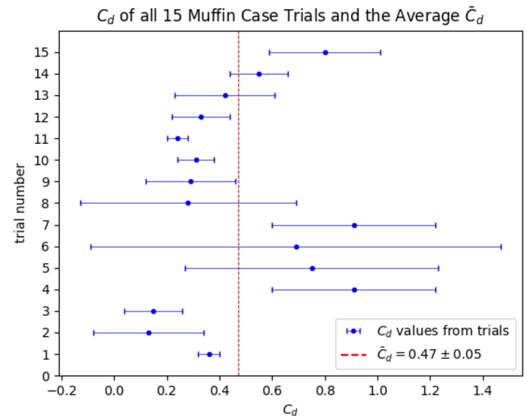

(b) Forest plot of measured C_d for muffin cases.

Figure 3: The distributions of measured C_d at different trials for both sponges and muffin cases. Average $\bar{C}_d$ is shown as a dashed red line.

The average $\bar{C}_d$ for sponges was calculated to be 1.08 ± 0.03. All sponges' C_d can be seen in Figure 3(a). The trail number increases with the combined mass of sponges in it. There's a noticeable shift to lower values of the coefficient as the number of sponges stacked together increases. This seems to be caused by a larger lateral surface, perhaps allowing the flow to stabilise on the sides and thus lowering the overall drag. Finally, the result can be compared to coefficients of drag of similar shapes. For a cube moving through a turbulent fluid with only one side exposed $C_d(\text{cube}) = 1.05$ [2]. This is reasonably close to the measured C_d for sponges, although one could expect it to be a bit higher since the rectangular face of a sponge is less symmetric. For example, a flat three-dimensional plate has a $C_d(\text{plate})$ of 1.28 [2]. Indeed, the fact that it is so close to the cube's coefficient suggests that the porous structure lowers the coefficient of drag, although more experiments would have to be performed to confirm this observation.

As for sponges, the $\bar{C}_d$ of muffin cases was calculated as an average, yielding the value of 0.47 ± 0.05. Again, all values can be seen in the forest plot in Figure 3(b), organised by the trial number in the same way as sponges. Unlike them, however, there does not seem to be any systemic shift in values as mass increases but rather a random distribution. This is to be expected as the overall shape hardly changes as the cases are stacked. In general, the uncertainty is reduced for higher masses where the weight force becomes stronger and Equation (8) works better at estimating g'. The low error in the first three points is likely an underestimation. Different error calculation approaches have been attempted and the partial differential method produced the largest error, which was still small. A comparison of the result to similar shapes is more difficult for muffin cases as there is no literature value for their C_d. Although, there is an argument to be made that the average $\bar{C}_d$ is too low by comparison with a cone, whose coefficient is usually given to be 0.5 [2]. Since a muffin case can be approximated as a cone with its tip cut off, one would expect the resulting C_d to be higher due to a flat portion of the frontal area. However, it is not clear what effect the ridges on the sides have. Therefore, it could be that the two characteristics essentially cancel each other out, leading the coefficients of a cone and a muffin case to be close in value.

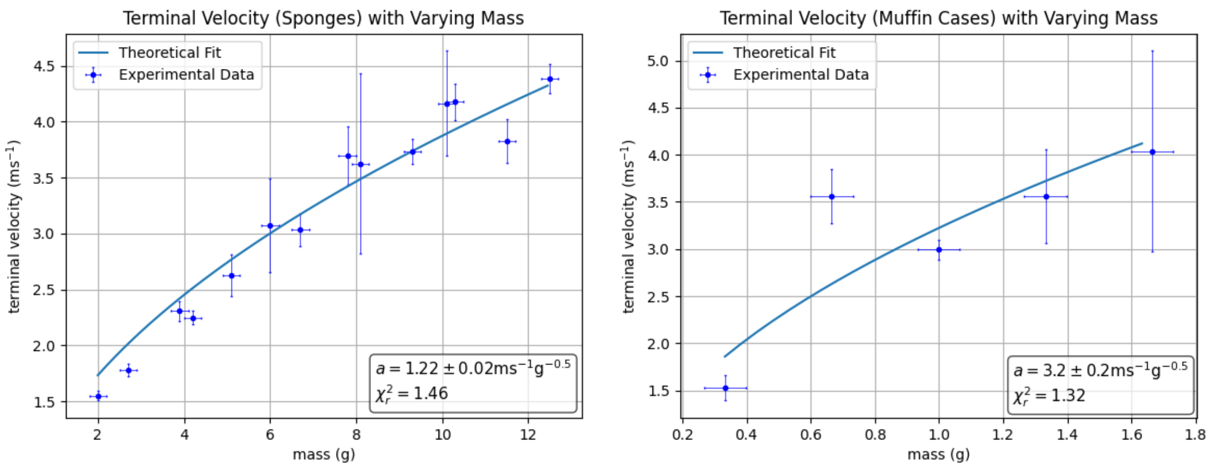

(a) Plot of terminal velocities for sponges.

(b) Plot of terminal velocities for muffin cases.

Figure 4: Plots of terminal velocity (m s^{-1}) against mass (g) obtained from the experiment.

Figure 4 shows the found relation of terminal velocity on mass. There are only 5 data points for muffin cases because the trials were averaged in each set, with error bars coming from the standard error. Equation (7) predicts a square-root dependence on mass where the coefficient depends on g', C_d, ρ and A. The theoretical functions seem to be good fits for the data in both plots, with χ_r^2 relatively close to 1. This supports the derived relation.

5 Conclusion

The observed free-fall of objects in the air is in good agreement with the theory of drag forces caused by turbulent fluid flow. The resulting coefficients of drag differ slightly from what would typically be expected from literature data. However, this can be attributed to the atypical choice of objects. More investigation could be conducted to find the effect of porous structure on C_d. The terminal velocity square-root dependence on mass is also largely in agreement with the results.

References

[1] Marcelle Size Knaack. “Encyclopedia of US Air Force Aircraft and Missile Systems”. In: Office of Air Force History, 1978, p. 285.

[2] F. Hoerner Sighard. “Fluid-Dynamic Drag”. In: Hoerner Fluid Dynamics, 1965. ISBN: 9991194444.

[3] Yasuki Nakayama et al. “Introduction to Fluid Mechanics”. In: Elsevier, 2018.